

RESEARCH ARTICLE

MICROSCOPY
RESEARCH TECHNIQUE

WILEY

Brain tumor detection and multi-classification using advanced deep learning techniques

Tariq Sadad¹ | Amjad Rehman² | Asim Munir³ | Tanzila Saba² |
Usman Tariq⁴ | Noor Ayesha⁵ | Rashid Abbasi⁶

¹Department of Computer Science, University of Central Punjab, Lahore, Pakistan

²Artificial Intelligence & Data Analytics Lab, CCIS Prince Sultan University, Riyadh, Saudi Arabia

³Department of Computer Science and Software Engineering, International Islamic University, Islamabad, Pakistan

⁴College of Computer Engineering and Science, Prince Sattam bin Abdulaziz University, Alkharj, Saudi Arabia

⁵School of Clinical Medicine, Zhengzhou University, Zhengzhou, Henan, China

⁶School of Information and Communication Engineering, University of Electronic Science and Technology of China, Chengdu, Sichuan, China

Correspondence

Usman Tariq, College of Computer Engineering and Science, Prince Sattam bin Abdulaziz University, Alkharj, Saudi Arabia.

Review Editor: Alberto Diaspro

Abstract

A brain tumor is an uncontrolled development of brain cells in brain cancer if not detected at an early stage. Early brain tumor diagnosis plays a crucial role in treatment planning and patients' survival rate. There are distinct forms, properties, and therapies of brain tumors. Therefore, manual brain tumor detection is complicated, time-consuming, and vulnerable to error. Hence, automated computer-assisted diagnosis at high precision is currently in demand. This article presents segmentation through Unet architecture with ResNet50 as a backbone on the Figshare data set and achieved a level of 0.9504 of the intersection over union (IoU). The preprocessing and data augmentation concept were introduced to enhance the classification rate. The multi-classification of brain tumors is performed using evolutionary algorithms and reinforcement learning through transfer learning. Other deep learning methods such as ResNet50, DenseNet201, MobileNet V2, and InceptionV3 are also applied. Results thus obtained exhibited that the proposed research framework performed better than reported in state of the art. Different CNN, models applied for tumor classification such as MobileNet V2, Inception V3, ResNet50, DenseNet201, NASNet and attained accuracy 91.8, 92.8, 92.9, 93.1, 99.6%, respectively. However, NASNet exhibited the highest accuracy.

Two processes of transfer learning: freeze and fine-tune, are performed to extract significant features from MRI slices. Brain tumor multi-classification is performed using transfer learning, ResNet50-UNet, and NASNet architecture.

KEYWORDS

brain tumor, cancer, health risks, healthcare, NASNet, WHO

1 | INTRODUCTION

Analysis and classification of medical imaging play an important role in detecting abnormalities in various body organs, such as blood cancer (Abbas, Saba, Mohamad, et al., 2018; Abbas, Saba, Rehman, et al., 2019; Abbas, Saba, Rehman, et al., 2019; Abbas, Saba, Mehmood, et al., 2019; Rehman, Abbas, Saba, Mahmood, & Kolivand, 2018; Rehman, Abbas, Saba, Rahman, et al., 2018; Rehman, Abbas, Saba, Mehmood, et al., 2018), lung cancer (Khan, Nazir,

et al., 2019; Saba, 2019; Saba, 2020; Saba, Sameh, Khan, Shad, & Sharif, 2019), brain tumor (Saba, Mohamed, El-Affendi, Amin, & Sharif, 2020), breast cancer (Marie-Sainte, Saba, Alsaleh, Alotaibi, & Bin, 2019; Mughal, Muhammad, Sharif, Rehman, & Saba, 2018; Mughal, Muhammad, Sharif, Saba, & Rehman, 2017; Mughal, Sharif, Muhammad, & Saba, 2018). Moreover, organ abnormalities often lead to rapid growth of tumors, which is the world's leading cause of death (Fahad, Khan, Saba, Rehman, & Iqbal, 2018; Saba, Al-Zahrani, & Rehman, 2012; Saba, Bokhari, Sharif, Yasmin, & Raza, 2018; Saba,

Rehman, Mehmood, Kolivand, & Sharif, 2018; Ullah et al., 2019; Yousaf, Mehmood, Saba, et al., 2019; Yousaf, Mehmood, Awan, et al., 2019).

Brain tumors are a deadly illness and are blamed for several deaths worldwide per year (Amin, Sharif, et al., 2020; Amin, Sharif, Raza, Saba, & Anjum, 2019; Amin, Sharif, Raza, Saba, & Rehman, 2019; Amin, Sharif, Rehman, Raza, & Mufti, 2018; Amin, Sharif, Yasmin, Saba, & Raza, 2019). Brain tumor appears in two kinds: benign and malignant. The benign tumor does not migrate to the surrounding tissues, but it is typically not life threatening. Malignant tumor, however, extends to other tissues and is thus harmful (WHO). WHO classifies brain tumors into four groups (I, II, III, and IV). The least of all classes is the pace at which the Grade I tumor spreads itself, while the Grade IV tumor is the most harmful and destructive (Ejaz et al., 2018, 2020; Ejaz, Rahim, Bajwa, Rana, & Rehman, 2019). For patients' clinical preparation, early identification of brain tumors is very critical (Iqbal et al., 2019; Iqbal, Ghani, Saba, & Rehman, 2018; Iqbal, Khan, Saba, & Rehman, 2017). It is possible to detect brain tumors either through diagnostic image processing or through biopsy. Per strategy has its own pros and cons. Practitioners often utilize both invasive and non-invasive brain tumor diagnostic methods depending on the case (Saba et al., 2020).

Various experimental imaging techniques, including CT and MRI, are used for cancer/ tumor diagnosis. However, relative to CT, MRI is safer because it does not subject living cells to toxic radiation (Afza, Khan, Sharif, & Rehman, 2019; Al-Ameen et al., 2015; Husham, Alkawaz, Saba, Rehman, & Alghamdi, 2016; Hussain et al., 2020; Javed, Rahim, & Saba, 2019; Javed, Rahim, Saba, & Rashid, 2019; Javed, Rahim, Saba, & Rehman, 2020; Javed, Saba, Shafry, & Rahim, 2020). Normally, patients perform a biopsy to assess the tumor's form and classification following early detection of abnormality using brain MRI. In this respect, the biopsy findings for detecting brain tumors are regarded as an absolute test. Different computer-aided diagnostic solutions have been suggested to increase brain tumor diagnosis precision, whether benign or malignant. For the classification of brain tumor grade, different researchers have used a range of unsupervised learning methods such as SVM, logistic regression, K-means, and supervised learning such as random forest classifier, artificial neural networks, and naïve Bayes. Some researchers also proposed a hybrid classification for the same task (Adeel et al., 2020; Iftikhar, Fatima, Rehman, Almazyad, & Saba, 2017; Jamal, Hazim Alkawaz, Rehman, & Saba, 2017; Khan, Sharif, et al., 2020; Khan, Akram, et al., 2020; Khan, Sharif, Yasmin, & Saba, 2017; Saba, 2017).

Currently, deep learning has outperformed conventional machine learning methods in several functions in recent years. Several deep learning approaches have also been used (Mittal et al., 2020; Qureshi, Khan, Sharif, Saba, & Ma, 2020; Ramzan, Khan, et al., 2020; Ramzan, Khan, Iqbal, Saba, & Rehman, 2020). For the role of brain tumor grade classification, several researchers have used pre-trained CNN architectures and fine-tuned them. Some have recommended modern architectures as well and taught them from scratch. 2D was the bulk of the CNNs used, although others have even used CNN architectures in 3D (Khan, Sharif, et al., 2019; Khan, Javed, Sharif, Saba, & Rehman, 2019; Rehman, Khan, Saba, et al., 2021).

The brain tumor classification task generally consists of four phases: preprocessing, tumor detection, features extraction & selection, classification of brain tumor grade (Khan, Lali, et al., 2019).

A novel Fidon et al. have proposed scalable multimodal deep learning architecture for brain tumor detection (2017) with dice scores of 0.77, 0.64, and 0.56 on BraTS 2013 data set. Seetha and Raja (2018) introduced a CNN framework for automatic brain tumor identification and detection. For brain tumor segmentation and texture, Fuzzy-C-means creates features isolated from segmented areas. Finally, these features are fed to fused DNN and SVM classifiers and have reached 97.5% accuracy. Khawaldeh et al. introduced a non-invasive graduation scheme of brain Glioma tumors (2018) using an updated version of AlexNet CNN. The regression was achieved for whole-brain MR images and image labeling was not pixel level, but with the image level. The experimental results show that a reasonable performance was achieved by 91.16% of the method. Sajjad et al. (2019) proposed a comprehensive method for brain tumor gradings. For this reason, the tumorous region after data augmentation was fed to pre-trained VGG-19 CNN. The rating accuracy 87.38 and 90.67%, respectively, stated for data before and after the augmentation. Özyurt, Sert, Avci, and Dogantekin (2019) fused CNN with the neuromorphic, optimistic entropy of the total fuzzy expert (NS-CNN) to evaluate brain tumors. These images were then applied to the CNN for feature extraction. Eventually, extracted features are fed in the SVM classification to be categorized as benign or malignant with an averaged 95.62% precision.

For brain tumor grading classification, Saba, Mohamed, et al. (2020) used the GrabCut technique to obtain MRI texture characteristics. Of note, 98.78, 99.63, and 99.67% accuracy recorded on (BraTS) of VGG-19 (CNN architecture) in 2015, 2016, and 2017, respectively. Ejaz et al. (2020) proposed using the MICCAI BraTS data set for hybrid SOM pixel marking with decreased cluster inclusion and deterministic function clustering to identify brain tumors. The cluster was collected utilizing three unsupervised learning methods for brain tumor segmentation. The system was tested using the dice overlap test, the Jaccard Tanimoto coefficient test, mean squared error, and peak signal to noise ratio. The findings obtained were 98%, 0.06, 18 lb, and 96%, respectively (Khan, Ashraf, et al., 2020).

Iqbal et al. (2019) have developed a deep learning model for brain tumor segmentation by combining short-term memory (LSTM) and coevolutionary neural networks (ConvNet). Of note, 75% ConvNet accuracy, 80% LSTM-based network accuracy, and 82.29% composite accuracy were recorded on the BraTS 2018 data set. Recently, for brain tumor detection, Rehman, Khan, Saba, et al. (2021) used pre-trained 3D CNN. Three BraTS databases were checked in 2015, 2017, and 2018, with 98.32, 96.97, and 92.67% precision.

1.1 | Main contributions

The main contributions of this research are as under

- In the preprocessing phase, a contrast-stretching algorithm is used to produce images of high-resolution.

- Brain tumor detection is performed through Unet architecture with ResNet50 as a backbone.
- The process of data augmentation is employed to achieve better results on small datasets.
- A new optimized framework called NASNet is applied, which uses the idea of Evolutionary Algorithms (EAs) and Reinforcement Learning (RL) for the optimization task.
- Finally, we also employed other deep transfer learning models such as ResNet50, DenseNet201, MobileNet V2 and InceptionV3 for brain tumor classification. We compared them with the NASNet Model to show the efficiency of NASNet model.

Further, this article is structured into different sections, Section 2 presents research background, Section 3 presents the proposed model with a detailed explanation of data set, preprocessing, ResNet50-UNet segmentation, NASNet model, data augmentation, and pseudo code. Section 4 highlighted the performance measures. Section 5 exhibits experimental results and Section 6 concludes research along with future directions.

2 | RESEARCH BACKGROUND

CNN has a prominent role in pattern and image recognition problems. CNN filters are convolved upon input image to extract features automatically. CNN architecture involves convolutional layers, pooling layers and fully connected layers and hidden layers based on architecture. The most common CNN architectures are AlexNet (Krizhevsky, Sutskever, & Hinton, 2012), VGGNet (Simonyan & Zisserman, 2015), MobileNet, DenseNet (DenseNet: Better CNN Model than ResNet, n. d.), Inception (Szegedy, Vanhoucke, Ioffe, Shlens, & Wojna, 2016), ResNet (He et al., 2016) and NASNet architecture (Radhika, Devika, Aswathi, & Padma, 2020). LeNet architecture introduced CNN's idea in 1990, but this architecture was not practical until 2010 due to limited computational resources. The notion of backpropagation was mainly presented by LeNet (LeCun, Bottou, Bengio, & Haffner, 1998). AlexNet was developed for object identification task and a deeper network than LeNet and it achieved better accuracy on ImageNet (Krizhevsky et al., 2012). Similarly, a filter size of 3×3 was introduced in all the types of VGGNet, such as VGG16 and VGG19 to learn nonlinear, complex features and make it computationally efficient. Furthermore, GoogLeNet tried to reduce the number of parameters and computations (Szegedy et al., 2015). The main aim of all the grown architectures focused on increasing depth of the model to enhance accuracy. This causes a vanishing gradient problem; during back propagation, the gradient generates too small a value, resulting in poor learning. ResNet proposed a solution to the vanishing gradient problem by employing skip functions to enhance the network's performance. A dense network has been produced for pattern reuse (DenseNet: Better CNN Model than ResNet, n.d.). For successful employment in embedded and mobile applications, a separable-convolution was introduced to reduce the number of parameters in MobileNet (Sandler, Howard, Zhu, Zhmoginov, & Chen, 2018). A new

optimized framework called NASNet was evolved, which employed the idea of EAs and RL for optimization tasks (Zoph, Vasudevan, Shlens, & Le, 2018). Based on the information obtained from the above-stated frameworks, we focused on NASNet architecture. The proposed research work uses search techniques to locate good convolutional architectures on a database of interest. The search methodology employed in the NASNet model is the Neural Architecture Search (NAS) framework introduced by (Zoph & Le, 2017). We employed NASNet and various transfer learning techniques for useful feature extraction, including ResNet50, DenseNet201, MobileNet V2 and InceptionV3 to achieve classification and detection on target data set. Furthermore, we compared the NASNet model with others architecture to show its efficacy. Besides, we could use proposed methodology in other domains to gain the advantages of this research activity.

2.1 | Ethical approval

No experiments are conducted on animals and humans. Only publicly available benchmark data sets are used for experiments.

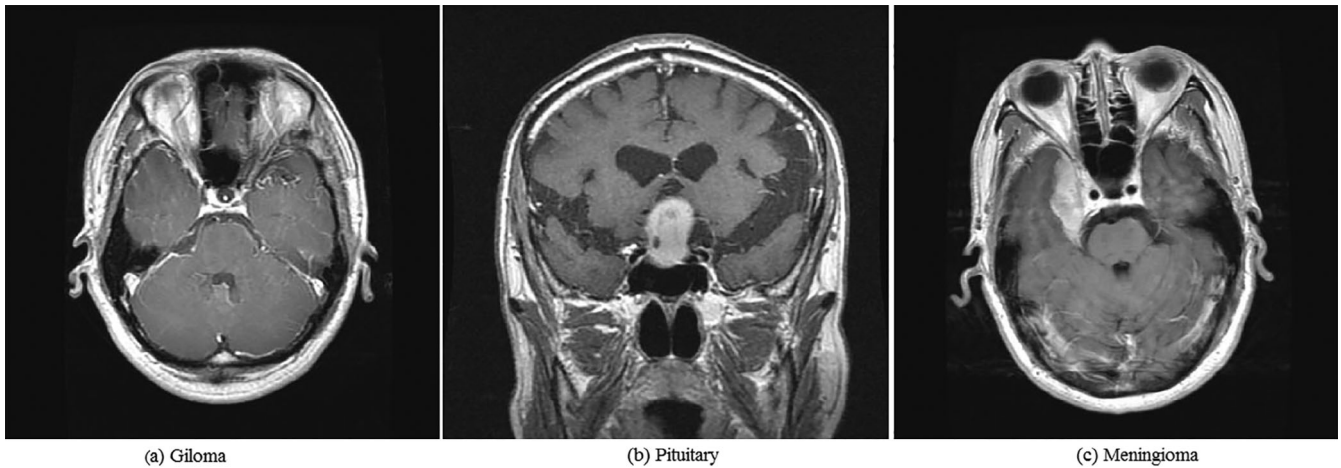
3 | PROPOSED MODEL FOR TUMOR DETECTION AND CLASSIFICATION

3.1 | Data sets

We employed a public brain tumor data set from Figshare source containing 3,064 brain MRI slices obtained from 233 patients (Cheng, 2017). It involves three brain tumors: glioma, pituitary, meningioma tumor and three distinct views: sagittal, axial, coronal views. The data set is available in ".mat" format. Each MAT-file covers a structure including patient ID, 512×512 image data in uint16 format, types of brain tumors, border of tumor with the coordinate's points, and ground truth in binary mask image. As CNN architecture takes the image, we only used image data from the .mat files in our experiment as presented in Figure 1. Furthermore, database description is depicted in Table 1 and the distribution of tumor types is presented in Figure 2.

3.2 | Preprocessing

Normally preprocessing is employed to improve and enhance the input data to smooth line further processing (Lung, Salam, Rehman, Rahim, & Saba, 2014; Majid et al., 2020; Marie-Sainte, Aburahmah, Almohaini, & Saba, 2019; Marie-Sainte, Saba, et al., 2019; Rehman, Khan, Mehmood, et al., 2020). In this case, it was mandatory since the MRI images were acquired from various modalities that involve artifacts. Therefore, various image processing methodologies were employed to enhance its contrast (Saba, Khan, Islam, et al., 2019; Saba, Khan, Rehman, & Marie-Sainte, 2019; Sadad, Munir, Saba, &



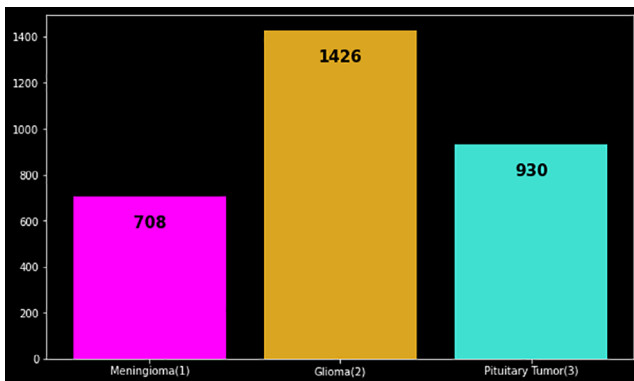
(a) Glioma

(b) Pituitary

(c) Meningioma

FIGURE 1 Brain tumor types**TABLE 1** Dataset description

Category	Patients	Number of slice
Glioma	91	1,426
Pituitary	60	930
Meningioma	82	708
Total	233	3,064

**FIGURE 2** Distribution of tumor type [Color figure can be viewed at wileyonlinelibrary.com]

Hussain, 2018). We applied the contrast-stretching algorithm to produce images of high-resolution using the following formula.

$$E(x, y) = \frac{i(x, y) - f_{\min}}{f_{\max} - f_{\min}}$$

where, f_{\min} and f_{\max} are the minimum [0] and maximum value [255] in the image $i(x, y)$ and x, y denote each pixel in the image.

Furthermore, we resized the input images into 224×224 as per the requirement of the proposed pre-trained models (Khan et al., 2019).

3.3 | Proposed model for brain tumor detection

In this article, we employed U-Net architecture (Ronneberger, Fischer, & Brox, 2015) for brain tumor detection, which achieved a remarkable efficiency in detecting medical images. The backbone applied is ResNet50 (He et al., 2016) which is pre-trained on the ImageNet data set. Thus, we employed U-Net model with ResNet50 as a backbone to obtain the best detection. Our ResNet50-U-Net segmentation architecture comprises an encoder and a decoder. The encoder is developed by eliminating the

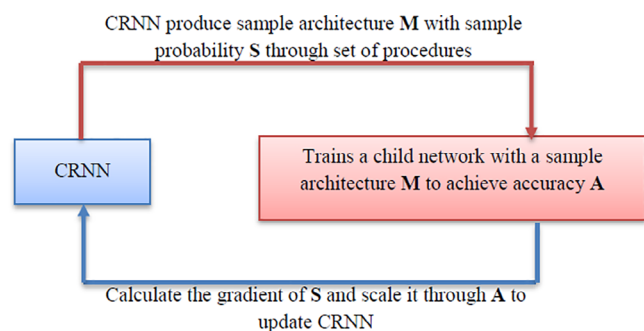
global average pooling and fully connected layer from the end of ResNet50. The decoder involves five blocks, every block containing 2×2 up-sampling layer subsequently two sets of layers, encompassing a convolution layer, Rectified Linear Unit (ReLU) and batch normalization layer. The parameters are not set by the architecture itself and could be performed through a fine-tuning approach. The weights and learning rate of ResNet50-U-Net architecture are loaded and initialized to train the model. Following parameters for ResNet50-U-Net segmentation are set as illustrated in Table 2.

3.4 | Proposed model for brain tumor classification

The idea of NASNet model is introduced by the Google ML group based on reinforcement learning. In NASNet, various amendments are performed depending upon weights, the number of layers, regularization procedures, and so forth, to enhance the architecture's efficiency. The framework of NASNet comprises of CNN and Controller Recurrent Neural Network (CRNN) described in Figure 3. As shown, a CRNN samples child architectures with various networks. The child networks are trained to get accuracy. The obtained accuracies are employed for controller updating so that the controller will produce improved networks over time. The weights of the controller are updated through gradient policy. The NASNet frameworks select the finest best cells through the reinforcement learning approach, as explained in (Zoph et al., 2018). Chen et al. (2018) documented that a

TABLE 2 Hyper-parameter for detection

Model	Unet
Backbone	ResNet50
Image size	256 × 256
Weight	ImageNet
Optimizer	Adam
Loss	bce_jaccard_loss
Metrics	iou_score
Epochs	80
Random seed	42
Batch size	16

**FIGURE 3** Controller Recurrent Neural Network in NASNet framework [Color figure can be viewed at wileyonlinelibrary.com]

reinforced evolutionary approach could be applied to choosing the best elements. A tournament selection approach is employed to reduce the poor performing cell. The fitness function of the child is improved and reinforcement mutations are accomplished. Through this activity, the performance of cell structure optimizes further.

The NASNet network is trained using two kinds of input images having size 224×224 and 331×331 , to achieve NASNet Mobile and NASNetLarge networks, respectively, presented in Table 3. Shifting from NASNetMobile to NASNetLarge requires a massive expansion in the number of parameters. Because NASNetLarge consist of 8,89,49,818 parameters and NASNetMobile comprises of 53,26,716 parameters. This creates NASNetMobile more consistent. In NASNet network, the smallest unit blocks, which are combined to create a cell as illustrated in Figure 4.

A cell is developed by concatenating various blocks, as presented in Figure 5. NASNet used a search space by factorizing the architecture into cells and further splitting it into blocks. The blocks and cells are flexible in type or number and are optimized for the specified database. More Detail about NASNet architecture can be found in (Liaqat et al., 2020; Mashood Nasir et al., 2020; Radhika et al., 2020).

The most vital accomplishments of CNNs are transfer learning that is employed where a smaller amount of data set is available such as the situation under study. In this research work, we have employed NASNet architecture for feature extraction and used ResNet50,

TABLE 3 The NASNet architecture

Identity	1×3 then 3×1 conv
1×7 then 7×1 conv	3×3 dilated conv
3×3 average pooling	3×3 max pooling
5×5 max pooling	7×7 max pooling
1×1 conv	3×3 conv
3×3 depthwise-separable-conv	5×5 depthwise-separable-conv
7×7 depthwise-separable-conv	

DenseNet201, MobileNet V2, and InceptionV3 to compare the results of NASNet with other used models. The significant features are extracted through two developments of transfer learning such as freeze layers and fine-tune. It means that the pre-trained architecture weights are transfer from source to target database, such as from ImageNet to Figshare in our case as illustrated in Figure 6. Fine-tuning of transfer learning is employed to enhance CNN architecture's efficacy and substitute the pre-trained model's final layers only. In simple words, 1,000 categories of ImageNet are substituted with the three kinds of brain tumor according to Figshare data set. In the proposed model, Adam optimizer is trained in each network, including NASNet and others for brain tumor classification. The batch size is set to 32 and $1e-4$ is assigned to the initial learn rate with the maximum epochs of 50 as presented in Table 4

3.5 | Data augmentation

For training purposes, deep learning approaches need vast volumes of labeled data. Unfortunately, the labeled medical image data set is not large enough, causing problems during training, especially utilizing deep learning methods (Nazir, Khan, Saba, & Rehman, 2019; Perveen et al., 2020; Saba, 2020). However, the data augmentation approach provides a remedy to this issue by increasing the size of the training data accessible. Therefore, the augmentation process is employed to achieve better results on a small data set. Various data augmentation styles, such as flipping and rotation, are applied to capable the architecture to learn the variations during training. The following parameters are employed during the augmentation process, as depicted in Table 5. Moreover, some sample images are illustrated in Figure 7.

3.6 | Pseudo codes for detection and classification

The pseudo codes for brain tumor detection and classification are presented as under.

1. procedure detection_type (brain tumor detection)

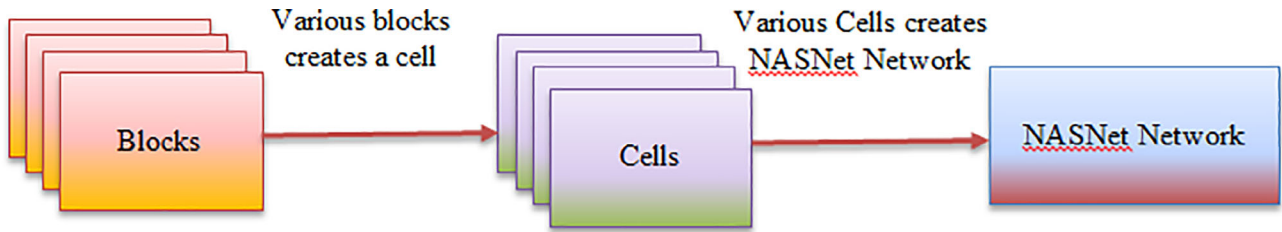


FIGURE 4 Creation of a cell in NASNet network [Color figure can be viewed at wileyonlinelibrary.com]

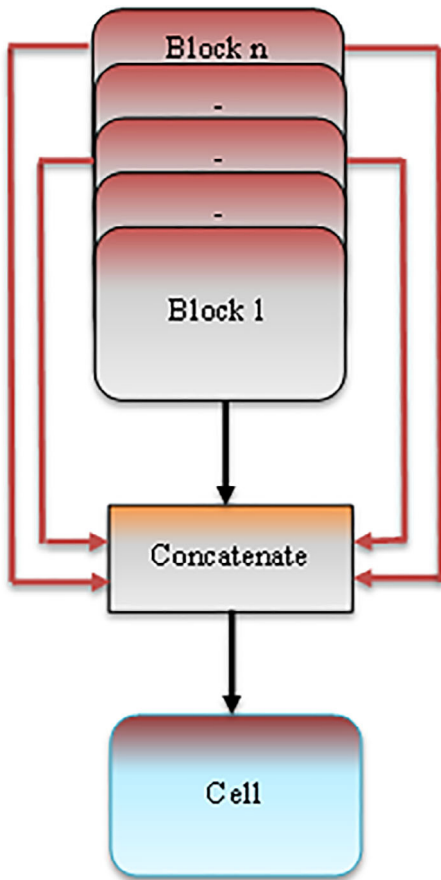


FIGURE 5 Arrangement of NASNet [Color figure can be viewed at wileyonlinelibrary.com]

- a. Input = Figshare_data set (3 types)
 - b. Unet_ResNet50 = detection (Input)
- return detection_type, IoU score
- 2. procedure classification (Figshare_data set, true class)
 - a. Model = training ((NASNet (Figshare_data set, trueclass, ImageNet))
 - b. Predicted_type = testing (Model (Figshare_data set))
 - c. Accuracy, Kappa = (Predicted_type, trueclass)
- return Predicted_type, Accuracy, Kappa, Confusion Matrix, ROC curve.

4 | PERFORMANCE MEASURE OF DETECTION AND CLASSIFICATION

The detection of tumors is evaluated through IoU to assess brain tumor detection accuracy on a Figshare data set. Similarly, the classification of networks' performance is evaluated through accuracy and Kappa statistic (κ) as recorded in Table 6. Kappa statistic (κ) is a measure of information employed to compares an observed accuracy with a predictable accuracy (Viera & Garrett, 2005). For further evaluation, the ROC curve and confusion matrix of the actual and predicted tumor class is calculated during the testing phase.

Where, True positive (TP), false positive (FP), true negative (TN), and false negative (FN) are concerned to show how much the applied model correctly and wrongly classified glioma, pituitary and meningioma tumors. Furthermore, t_0 is the relative experimental understanding between the ground truth and classification algorithm. The speculative probability of agreement chance by using comparative information to highlight the possibilities of every category.

5 | EXPERIMENTAL RESULTS

The experiments are carried on Google Colab services and performed based on the holdout method. We have assessed the best available brain tumor detection parameters using ResNet50-UNet architecture and achieved the highest IoU score of 0.9504 as presented in Figure 8. Furthermore, the actual and predicted mask is presented in Figure 9. We split the data set into two portions: training data involves 80% and testing data comprises 20% of the data set. We have evaluated the best parameters to get the highest performance of the architecture. The NASNet architecture generates the highest accuracy of 99.6% as compared to others. This value signifies the efficacy of NASNet architecture for feature extraction and classification of detected brain tumors. Similarly, the high value of kappa statistic of 0.99 for the NASNet network determines an ideal agreement with the ground truth, as presented in Table 7. Figure 10 indicates the confusion matrix acquired through the NASNet model for brain tumors classification.

The statistical validation of NASNet architecture is done through ROC analysis. Figure 11 presents the parameters for NASNet model with the resulting AUC value.

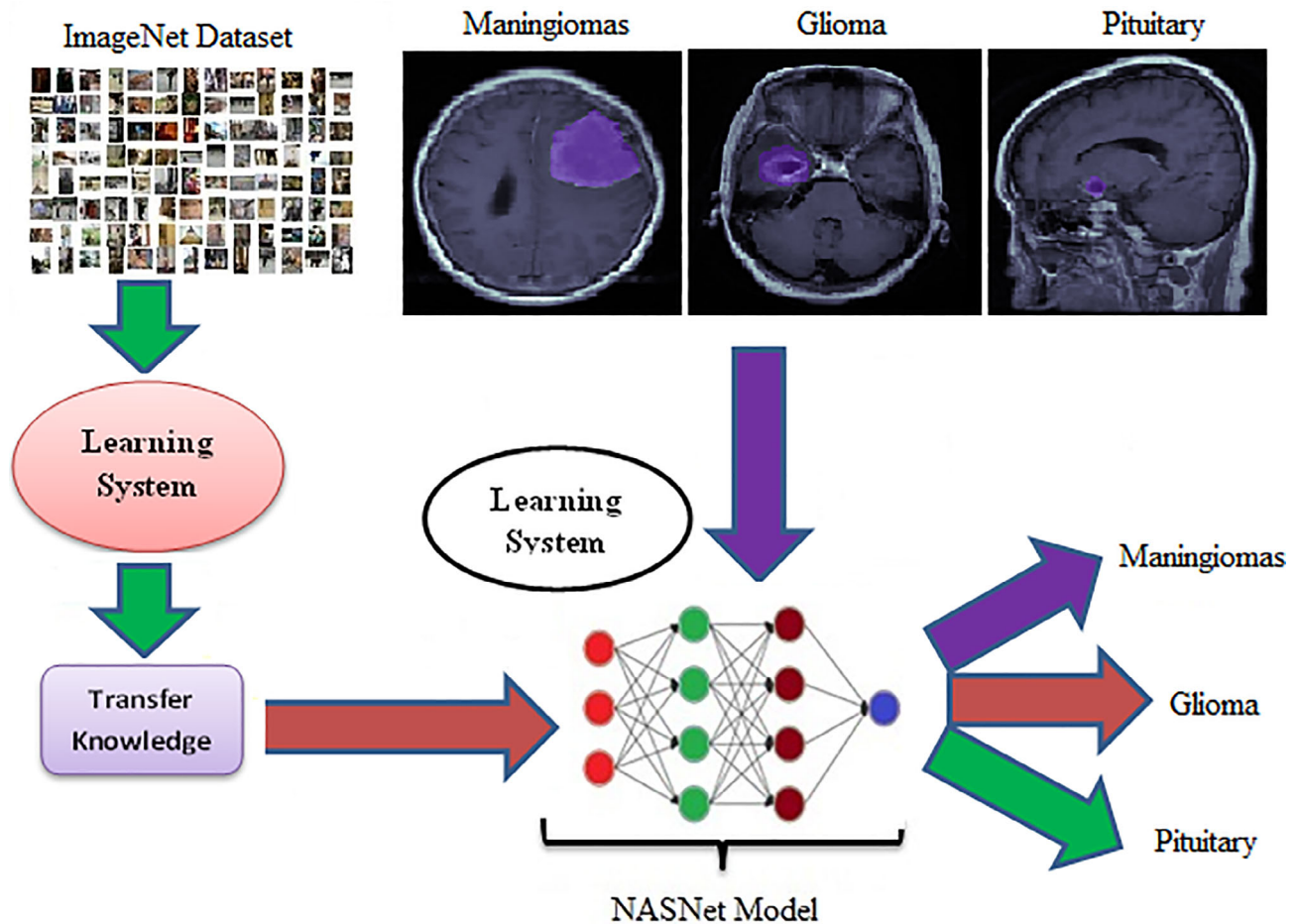


FIGURE 6 Proposed model [Color figure can be viewed at wileyonlinelibrary.com]

TABLE 4 Hyper-parameter for classification

Hyper-parameters	Value	Size of input image
Optimizer	Adam	224 × 224
Loss	Categorical crossentropy	
Batch size	32	
Pooling	GlobalAveragePooling2D	
Initial learning rate	1e-4	
Epoch	50	
Dropout	0.5	
Train size	0.8	
Test size	0.2	
Random state	11	

In Figure 12, we investigated the NASNet network's performance with DenseNet20, ResNet50, Inception V3, and MobileNet V2. We have noticed that NASNet model achieve high accuracy in term of classification.

TABLE 5 Data augmentation parameters

Parameters	Value
Horizontal flip	True
Vertical flip	True
Rotation range	90, 180

5.1 | Analysis and comparisons

Nonetheless, it is hard to compare the results with the techniques reported in state of the art due to different CNN models and data set employed (Khan, Jabeen, et al., 2020). However, we still compare current techniques on brain tumor detection and classification. Sajjad et al. (2019), after comprehensive data augmentation, fed tumor region to pre-trained VGG-19 CNN, which was fine-tuned for brain tumor grade classification and attained an accuracy of 90.67% with augmentation and without augmentation 87.38% on the radiopaedia data set.

For the classification of multimodal automatic brain tumors with linear contrast stretching, the transformation of learning-based

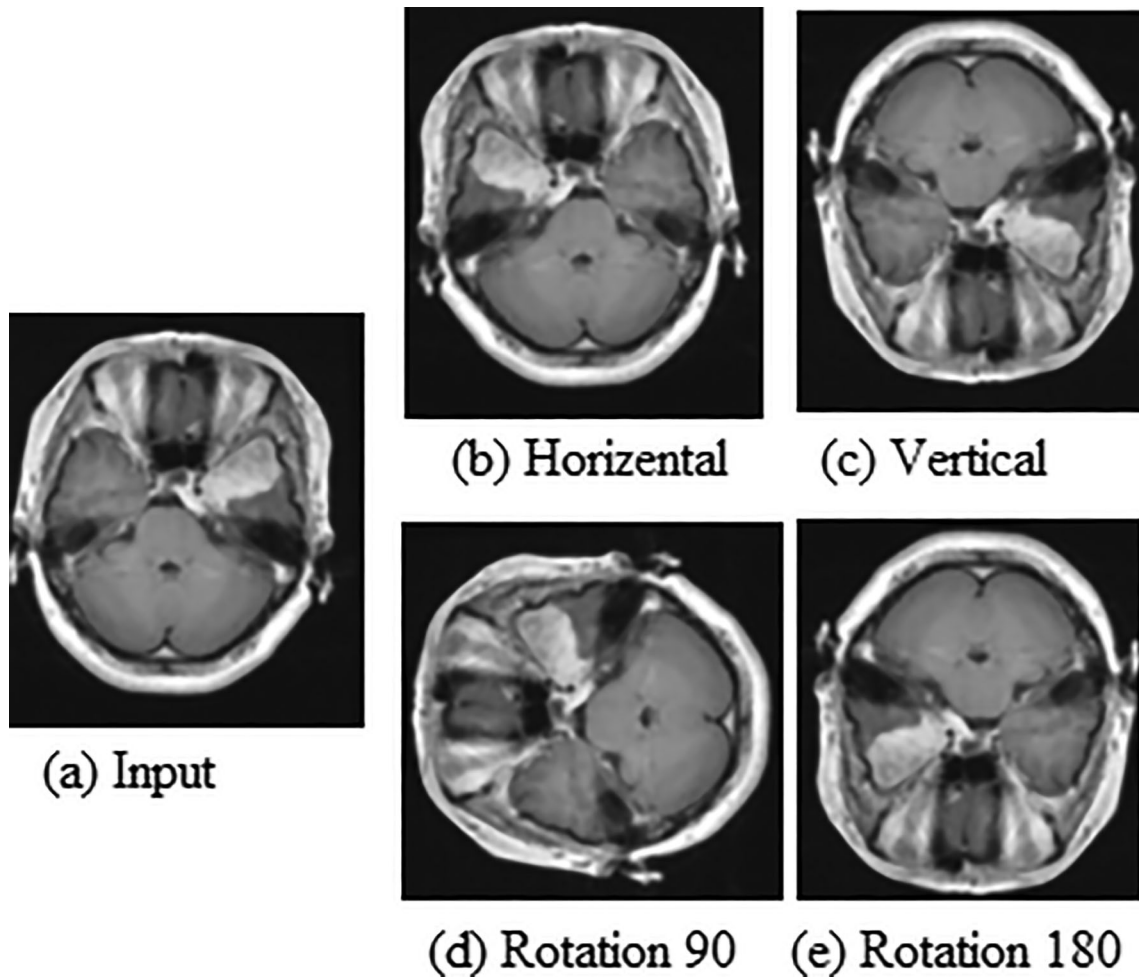


FIGURE 7 Data augmentation illustration

TABLE 6 Performance metrics

Measure	Formula
Accuracy	$\frac{TP+TN}{\{(TP+FN)+(FP+TN)\}}$
Kappa (κ)	$\frac{t_p - t_e}{1 - t_e}$

extraction functions, correntropy-based features set, Khan, Jabeen, et al. (2020) proposed a fusion of pre-trained CNN models (VGG16–VGG19). The fused matrix was eventually fed to the extreme learning machine for brain tumor identification. The suggested technique obtained an accuracy of 97.8, 96.9, and 92.5%, respectively, for BraTs2015, BraTs2017, and BraTs2018.

Recently, a 3D CNN architecture was developed by Rehman, Khan, Saba, et al. (2021) to identify brain tumors using a pre-trained CNN model and recorded an accuracy of 98.32, 96.97, and 92.67% in BraTs2015, BraTs2017, and BraTs2018.

Table 7 exhibits experimental results using different deep learning models to classify the brain tumor following its detection.

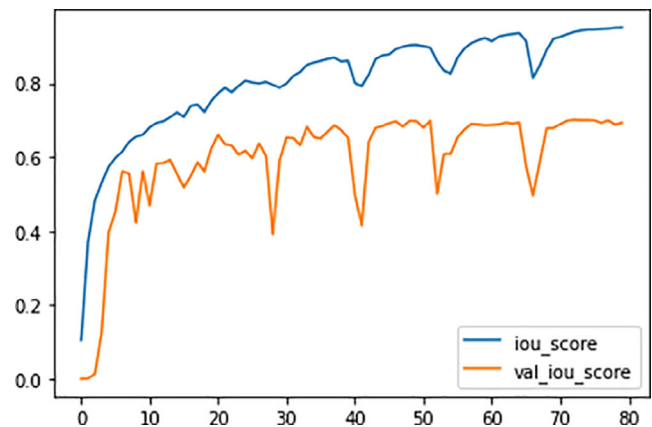
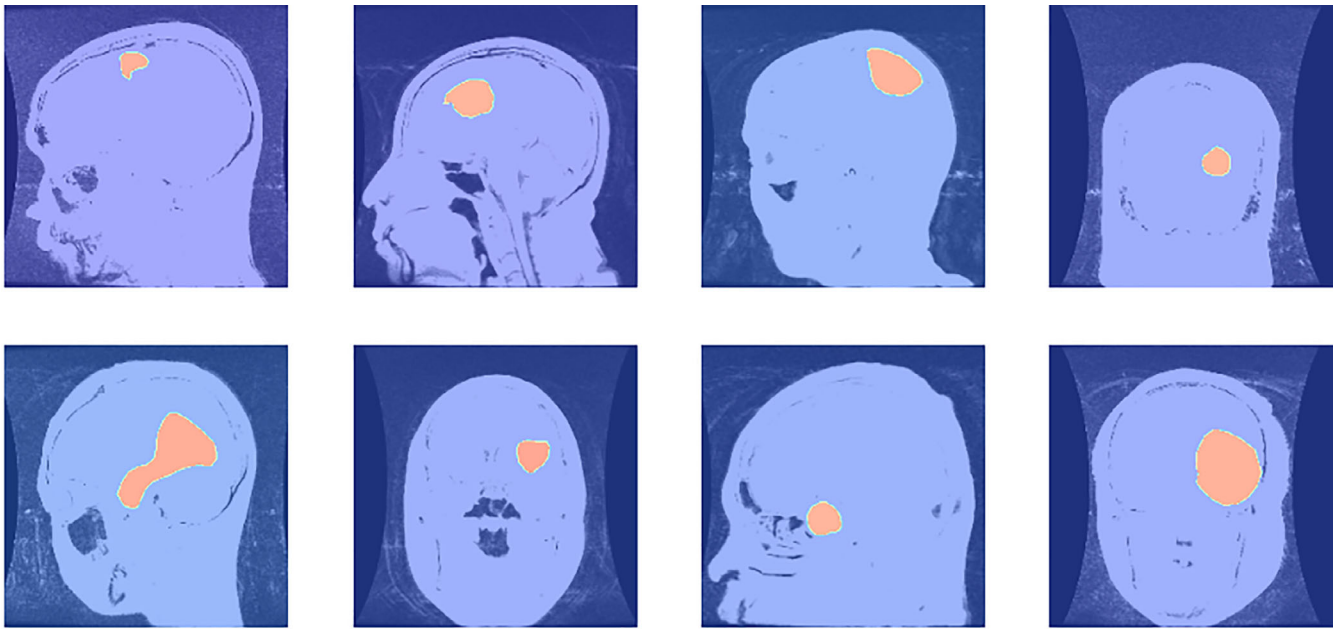


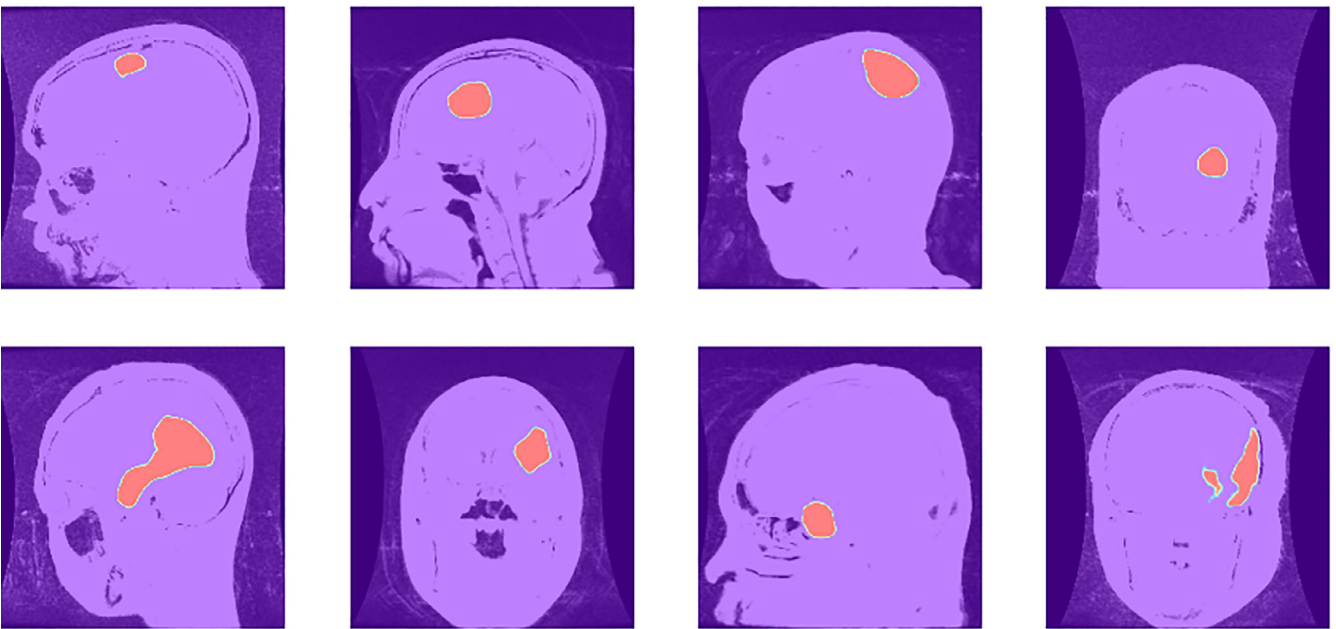
FIGURE 8 Analysis of tumor detection [Color figure can be viewed at wileyonlinelibrary.com]

6 | CONCLUSION

To explore and evaluate employed networks' performance, two transfer learning processes that are freeze and fine-tune, are performed in



(a) Actual



(b) Predicted

FIGURE 9 Actual versus predicted mask [Color figure can be viewed at wileyonlinelibrary.com]**TABLE 7** Experimental result

Task	Models	Accuracy	Kappa statistics
Classification of glioma, pituitary, and meningioma tumors	NASNet	99.6	0.99
	DenseNet201	93.1	0.89
	ResNet50	92.9	0.89
	Inception V3	92.8	0.88
	MobileNet V2	91.8	0.87

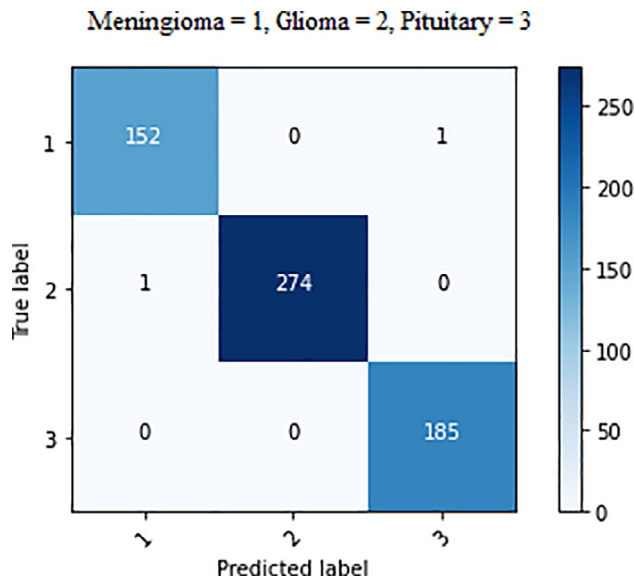


FIGURE 10 Confusion matrix of classification [Color figure can be viewed at [wileyonlinelibrary.com](https://onlinelibrary.com)]

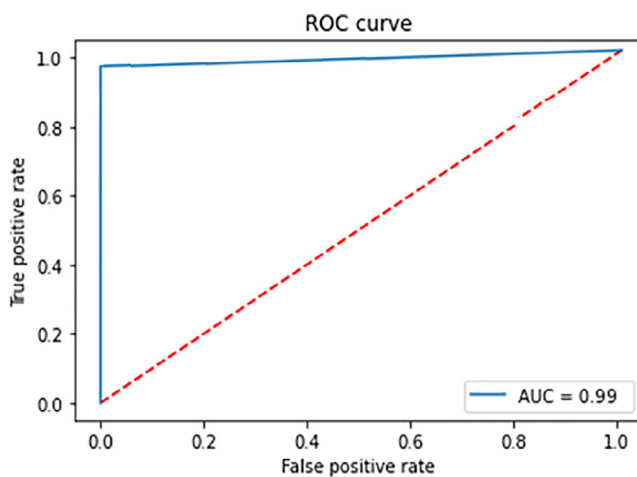


FIGURE 11 ROC curve of classification [Color figure can be viewed at [wileyonlinelibrary.com](https://onlinelibrary.com)]

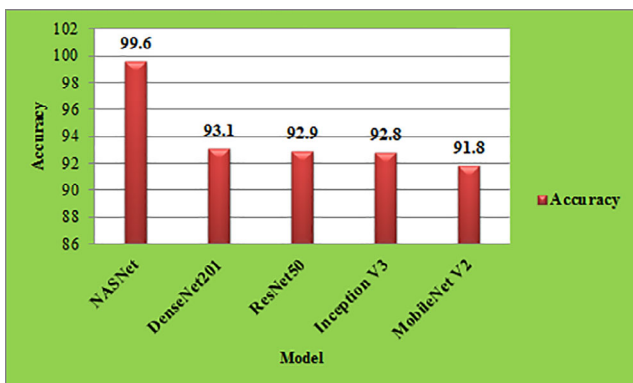


FIGURE 12 Performance analysis of classification [Color figure can be viewed at [wileyonlinelibrary.com](https://onlinelibrary.com)]

this article to extract significant features from MRI slices. A well-known segmentation technique such as Unet architecture with ResNet50 as a backbone to expose the tumor part and achieved 0.9504 of IoU score. Furthermore, multi-classification of brain tumor has been performed on Figshare data set to identify the tumor type. The process of multi-classification is performed using transfer learning and NASNet architecture. To show the efficacy of NASNet architecture compared with other architectures like ResNet50, DenseNet201, MobileNet V2, Inception V2 are executed. NASNet architecture achieved a higher classification accuracy of 99.6% on the target data set.

Although this research investigated various architectures of deep CNN with transfer learning for brain tumor detection, more models still need to be researched. Therefore, powerful architecture with less computational complexity will be employed in the future.

FUNDING

No specific funding received for this research.

ACKNOWLEDGMENT

This work was supported by Artificial Intelligence and Data Analytics (AIDA) Lab CCIS Prince Sultan University Riyadh, Saudi Arabia.

CONFLICT OF INTEREST

Authors declare that they have no conflict of interest and contribute scientifically equally to deserve authorship.

DATA AVAILABILITY STATEMENT

The data that support the findings of this study are openly available in [Figshare] at [<https://figshare.com/>], reference number [Brain tumor dataset]

ORCID

Tariq Sadad <https://orcid.org/0000-0002-0078-7849>

Amjad Rehman <https://orcid.org/0000-0002-3817-2655>

Tanzila Saba <https://orcid.org/0000-0003-3138-3801>

Usman Tariq <https://orcid.org/0000-0001-7672-1187>

Noor Ayesha <https://orcid.org/0000-0003-1439-3418>

REFERENCES

- Abbas, A., Saba, T., Rehman, A., Mehmood, Z., Javaid, N., Tahir, M., ... Shah, R. (2019). Plasmodium species aware based quantification of malaria, parasitemia in light microscopy thin blood smear. *Microscopy Research and Technique*, 82(7), 1198–1214. <https://doi.org/10.1002/jemt.23269>
- Abbas, N., Saba, T., Mehmood, Z., Rehman, A., Islam, N., & Ahmed, K. T. (2019). An automated nuclei segmentation of leukocytes from microscopic digital images. *Pakistan Journal of Pharmaceutical Sciences*, 32(5), 2123–2138.
- Abbas, N., Saba, T., Mohamad, D., Rehman, A., Almazyad, A. S., & Al-Ghamdi, J. S. (2018). Machine aided malaria parasitemia detection in Giemsa-stained thin blood smears. *Neural Computing and Applications*, 29(3), 803–818. <https://doi.org/10.1007/s00521-016-2474-6>
- Abbas, N., Saba, T., Rehman, A., Mehmood, Z., Kolivand, H., Uddin, M., & Anjum, A. (2019). Plasmodium life cycle stage classification-based

- quantification of malaria parasitaemia in thin blood smears. *Microscopy Research and Technique*. [https://doi.org/10.1002/jemt.2317082\(3\):283-295](https://doi.org/10.1002/jemt.2317082(3):283-295).
- Adeel, A., Khan, M. A., Akram, T., Sharif, A., Yasmin, M., Saba, T., & Javed, K. (2020). Entropy-controlled deep features selection framework for grape leaf diseases recognition. *Expert Systems*.
- Afza, F., Khan, M. A., Sharif, M., & Rehman, A. (2019). Microscopic skin laceration segmentation and classification: A framework of statistical normal distribution and optimal feature selection. *Microscopy Research and Technique*, 82(9), 1471-1488.
- Al-Ameen, Z., Sulong, G., Rehman, A., Al-Dhelaan, A., Saba, T., & Al-Rodhaan, M. (2015). An innovative technique for contrast enhancement of computed tomography images using normalized gamma-corrected contrast-limited adaptive histogram equalization. *EURASIP Journal on Advances in Signal Processing*, 32. <https://doi.org/10.1186/s13634-015-0214-1>
- Amin, J., Sharif, M., Raza, M., Saba, T., & Anjum, M. A. (2019). Brain tumor detection using statistical and machine learning method. *Computer Methods and Programs in Biomedicine*, 177, 69-79.
- Amin, J., Sharif, M., Raza, M., Saba, T., & Rehman, A. (2019). Brain tumor classification: Feature fusion. *2019 international conference on computer and information sciences (ICCIS)* (pp. 1-6). IEEE.
- Amin, J., Sharif, M., Raza, M., Saba, T., Sial, R., & Shad, S. A. (2020). Brain tumor detection: A long short-term memory (LSTM)-based learning model. *Neural Computing and Applications*. 32 15965-15973.
- Amin, J., Sharif, M., Rehman, A., Raza, M., & Mufti, M. R. (2018). Diabetic retinopathy detection and classification using hybrid feature set. *Microscopy Research and Technique*, 81(9), 990-996.
- Amin, J., Sharif, M., Yasmin, M., Saba, T., & Raza, M. (2019). Use of machine intelligence to conduct analysis of human brain data for detection of abnormalities in its cognitive functions. *Multimedia Tools and Applications*, 79(15), 10955-10973. <https://doi.org/10.1007/s11042-019-7324-y>
- Chen, Y., Meng, G., Zhang, Q., Xiang, S., Huang, C., Mu, L., & Wang, X. (2018). Reinforced Evolutionary Neural Architecture Search, arXiv preprint.
- Cheng, J. (2017). Brain tumor dataset. *Figshare*. <https://doi.org/10.6084/m9.figshare.1512427.v5>
- DenseNet: Better CNN Model than ResNet (n.d.). Retrieved from <http://www.programmingsought.com/article/%0A7780717554/>
- Ejaz, K., Rahim, M. S. M., Bajwa, U. I., Chaudhry, H., Rehman, A., & Ejaz, F. (2020). Hybrid segmentation method with confidence region detection for tumor identification. *IEEE Access*. <https://doi.org/10.1109/ACCESS.2020.3016627>
- Ejaz, K., Rahim, M. S. M., Bajwa, U. I., Rana, N., & Rehman, A. (2019). An unsupervised learning with feature approach for brain tumor segmentation using magnetic resonance imaging. *Proceedings of the 2019 9th International Conference on Bioscience, Biochemistry and Bioinformatics* (pp. 1-7).
- Ejaz, K., Rahim, M. S. M., Rehman, A., Chaudhry, H., Saba, T., & Ejaz, A. (2018). Segmentation method for pathological brain tumor and accurate detection using MRI. *International Journal of Advanced Computer Science and Applications*, 9(8), 394-401.
- Fahad, H. M., Khan, M. U. G., Saba, T., Rehman, A., & Iqbal, S. (2018). Microscopic abnormality classification of cardiac murmurs using ANFIS and HMM. *Microscopy Research and Technique*, 81(5), 449-457. <https://doi.org/10.1002/jemt.22998>
- He, K., Zhang, X., Ren, S., & Sun, J. (2016). Deep residual learning for image recognition. In *Proceedings of the IEEE conference on computer vision and pattern recognition* (pp. 770-778).
- Husham, A., Alkawaz, M. H., Saba, T., Rehman, A., & Alghamdi, J. S. (2016). Automated nuclei segmentation of malignant using level sets. *Microscopy Research and Technique*, 79(10), 993-997. <https://doi.org/10.1002/jemt.22733>
- Hussain, N., Khan, M. A., Sharif, M., Khan, S. A., Albeshar, A. A., Saba, T., & Armaghan, A. (2020). A deep neural network and classical features-based scheme for objects recognition: An application for machine inspection. *Multimedia Tools and Applications*. <https://doi.org/10.1007/s11042-020-08852-3>
- Iftikhar, S., Fatima, K., Rehman, A., Almazyad, A. S., & Saba, T. (2017). An evolution-based hybrid approach for heart diseases classification and associated risk factors identification. *Biomedical Research*, 28(8), 3451-3455.
- Iqbal, S., Ghani, M. U., Saba, T., & Rehman, A. (2018). Brain tumor segmentation in multi-spectral MRI using convolutional neural networks (CNN). *Microscopy Research and Technique*, 81(4), 419-427. <https://doi.org/10.1002/jemt.22994>
- Iqbal, S., Khan, M.U.G., Saba, T. Mehmood, Z. Javaid, N., Rehman, A., Abbasi, R. (2019) Deep learning model integrating features and novel classifiers fusion for brain tumor segmentation, *Microscopy Research and Technique*, 82(8); 1302-1315, <https://doi.org/10.1002/jemt.23281>
- Iqbal, S., Khan, M. U. G., Saba, T., & Rehman, A. (2017). Computer assisted brain tumor type discrimination using magnetic resonance imaging features. *Biomedical Engineering Letters*, 8(1), 5-28. <https://doi.org/10.1007/s13534-017-0050-3>
- Jamal, A., Hazim Alkawaz, M., Rehman, A., & Saba, T. (2017). Retinal imaging analysis based on vessel detection. *Microscopy Research and Technique 2017*, 80(17), 799-811. <https://doi.org/10.1002/jemt>
- Javed, R., Rahim, M. S. M., & Saba, T. (2019). An improved framework by mapping salient features for skin lesion detection and classification using the optimized hybrid features. *International Journal of Advanced Trends in Computer Science and Engineering*, 8(1), 95-101.
- Javed, R., Rahim, M. S. M., Saba, T., & Rashid, M. (2019). Region-based active contour JSEG fusion technique for skin lesion segmentation from dermoscopic images. *Biomedical Research*, 30(6), 1-10.
- Javed, R., Rahim, M. S. M., Saba, T., & Rehman, A. (2020). A comparative study of features selection for skin lesion detection from dermoscopic images. *Network Modeling Analysis in Health Informatics and Bioinformatics*, 9(1), 4.
- Javed, R., Saba, T., Shafry, M., Rahim, M. (2020). An Intelligent Saliency Segmentation Technique and Classification of Low Contrast Skin Lesion Dermoscopic Images Based on Histogram Decision. *2019 12th International Conference on Developments in eSystems Engineering (DeSE)* (pp. 164-169).
- Khan, M. A., Akram, T., Sharif, M., Javed, K., Raza, M., & Saba, T. (2020). An automated system for cucumber leaf diseased spot detection and classification using improved saliency method and deep features selection. *Multimedia Tools and Applications*, 1-30.
- Khan, M. A., Akram, T., Sharif, M., Saba, T., Javed, K., Lali, I. U., ... Rehman, A. (2019). Construction of saliency map and hybrid set of features for efficient segmentation and classification of skin lesion. *Microscopy Research and Technique*, 82(5), 741-763. <http://doi.org/10.1002/jemt.23220>
- Khan, M. A., Ashraf, I., Alhaisoni, M., Damaševičius, R., Scherer, R., Rehman, A., & Bukhari, S. A. C. (2020). Multimodal brain tumor classification using deep learning and robust feature selection: A machine learning application for radiologists. *Diagnostics*, 10, 565.
- Khan, M. A., Javed, M. Y., Sharif, M., Saba, T., & Rehman, A. (2019). Multi-model deep neural network-based features extraction and optimal selection approach for skin lesion classification. *2019 international conference on computer and information sciences (ICCIS)* (pp. 1-7). IEEE.
- Khan, M. A., Lali, I. U., Rehman, A., Ishaq, M., Sharif, M., Saba, T., ... Akram, T. (2019). Brain tumor detection and classification: A framework of marker-based watershed algorithm and multilevel priority features selection. *Microscopy Research and Technique*, 82(6), 909-922. <https://doi.org/10.1002/jemt.23238>
- Khan, M. A., Sharif, M., Akram, T., Raza, M., Saba, T., & Rehman, A. (2020). Hand-crafted and deep convolutional neural network features fusion and selection strategy: An application to intelligent human action recognition. *Applied Soft Computing*, 87, 105986.

- Khan, M. A., Sharif, M. I., Raza, M., Anjum, A., Saba, T., & Shad, S. A. (2019). Skin lesion segmentation and classification: A unified framework of deep neural network features fusion and selection. *Expert Systems*, e12497.
- Khan, M. W., Sharif, M., Yasmin, M., & Saba, T. (2017). CDR based glaucoma detection using fundus images: A review. *International Journal of Applied Pattern Recognition*, 4(3), 261–306.
- Khan, M. Z., Jabeen, S., Khan, M. U. G., Saba, T., Rehmat, A., Rehman, A., & Tariq, U. (2020). A realistic image generation of face from text description using the fully trained generative adversarial networks. *IEEE Access*.
- Khan, S. A., Nazir, M., Khan, M. A., Saba, T., Javed, K., Rehman, A., ... Awais, M. (2019). Lungs nodule detection framework from computed tomography images using support vector machine. *Microscopy Research and Technique*, 82(8), 1256–1266.
- Krizhevsky, A., Sutskever, I., & Hinton, G. E. (2012). ImageNet classification with deep convolutional neural networks. *Advances in Neural Information Processing Systems*.
- LeCun, Y., Bottou, L., Bengio, Y., & Haffner, P. (1998). Gradient-based learning applied to document recognition. *Proceedings of the IEEE*, 86, 2278–2324. <https://doi.org/10.1109/5.726791>
- Liaqat, A., Khan, M. A., Sharif, M., Mittal, M., Saba, T., Manic, K. S., & Al Attar, F. N. H. (2020). Gastric tract infections detection and classification from wireless capsule endoscopy using computer vision techniques: A review. *Current Medical Imaging*.
- Lung, J. W. J., Salam, M. S. H., Rehman, A., Rahim, M. S. M., & Saba, T. (2014). Fuzzy phoneme classification using multi-speaker vocal tract length normalization. *IETE Technical Review*, 31(2), 128–136. <https://doi.org/10.1080/02564602.2014.892669>
- Majid, A., Khan, M. A., Yasmin, M., Rehman, A., Yousafzai, A., & Tariq, U. (2020). Classification of stomach infections: A paradigm of convolutional neural network along with classical features fusion and selection. *Microscopy Research and Technique*, 83(5), 562–576.
- Marie-Sainte, S. L., Aburahmah, L., Almohaini, R., & Saba, T. (2019). Current techniques for diabetes prediction: Review and case study. *Applied Sciences*, 9(21), 4604.
- Marie-Sainte, S. L., Saba, T., Alsaleh, D., Alotaibi, A., & Bin, M. (2019). An improved strategy for predicting diagnosis, survivability, and recurrence of breast cancer. *Journal of Computational and Theoretical Nanoscience*, 16(9), 3705–3711.
- Mashood Nasir, I., Attique Khan, M., Alhaisoni, M., Saba, T., Rehman, A., & Iqbal, T. (2020). A hybrid deep learning architecture for the classification of superhero fashion products: An application for medical-tech classification. *Computer Modeling in Engineering & Sciences*, 124(3), 1017–1033.
- Mittal, A., Kumar, D., Mittal, M., Saba, T., Abunadi, I., Rehman, A., & Roy, S. (2020). Detecting pneumonia using convolutions and dynamic capsule routing for chest X-ray images. *Sensors*, 20(4), 1068.
- Mughal, B., Muhammad, N., Sharif, M., Rehman, A., & Saba, T. (2018). Removal of pectoral muscle based on topographic map and shape-shifting silhouette. *BMC Cancer*, 18(1), 1–14.
- Mughal, B., Muhammad, N., Sharif, M., Saba, T., & Rehman, A. (2017). Extraction of breast border and removal of pectoral muscle in wavelet domain. *Biomedical Research*, 28(11), 5041–5043.
- Mughal, B., Sharif, M., Muhammad, N., & Saba, T. (2018). A novel classification scheme to decline the mortality rate among women due to breast tumor. *Microscopy Research and Technique*, 81(2), 171–180.
- Nazir, M., Khan, M. A., Saba, T., & Rehman, A. (2019). Brain tumor detection from MRI images using multi-level wavelets. 2019, *IEEE International Conference on Computer and Information Sciences (ICIS)* (pp. 1–5).
- Özyurt, F., Sert, E., Avci, E., & Dogantekin, E. (2019). Brain tumor detection based on convolutional neural network with neutrosophic expert maximum fuzzy sure entropy. *Measurement*, 147, 106830.
- Perveen, S., Shahbaz, M., Saba, T., Keshavjee, K., Rehman, A., & Guergachi, A. (2020). Handling irregularly sampled longitudinal data and prognostic modeling of diabetes using machine learning technique. *IEEE Access*, 8, 21875–21885.
- Qureshi, I., Khan, M. A., Sharif, M., Saba, T., & Ma, J. (2020). Detection of glaucoma based on cup-to-disc ratio using fundus images international. *Journal of Intelligent Systems Technologies and Applications*, 19(1), 1–16. <https://doi.org/10.1504/IJISTA.2020.105172>
- Radhika, K., Devika, K., Aswathi, T., & Padma, S. Switzerland: (2020). Performance analysis of NASNet on unconstrained ear recognition. In *Studies in Computational Intelligence*. https://doi.org/10.1007/978-3-030-33820-6_3
- Ramzan, F., Khan, M. U. G., Iqbal, S., Saba, T., & Rehman, A. (2020). Volumetric segmentation of brain regions from MRI scans using 3D convolutional neural networks. *IEEE Access*, 8, 103697–103709.
- Ramzan, F., Khan, M. U. G., Rehmat, A., Iqbal, S., Saba, T., Rehman, A., & Mehmood, Z. (2020). A deep learning approach for automated diagnosis and multi-class classification of Alzheimer's disease stages using resting-state fMRI and residual neural networks. *Journal of Medical Systems*, 44(2), 37.
- Rehman, A., Abbas, N., Saba, T., Mahmood, T., & Kolivand, H. (2018). Rouleaux red blood cells splitting in microscopic thin blood smear images via local maxima, circles drawing, and mapping with original RBCs. *Microscopic Research and Technique*, 81(7), 737–744. <https://doi.org/10.1002/jemt.23030>
- Rehman, A., Abbas, N., Saba, T., Mehmood, Z., Mahmood, T., & Ahmed, K. T. (2018). Microscopic malaria parasitemia diagnosis and grading on benchmark datasets. *Microscopic Research and Technique*, 81(9), 1042–1058. <https://doi.org/10.1002/jemt.23071>
- Rehman, A., Abbas, N., Saba, T., Rahman, S. I. U., Mehmood, Z., & Kolivand, K. (2018). Classification of acute lymphoblastic leukemia using deep learning. *Microscopy Research and Technique*, 81(11), 1310–1317. <https://doi.org/10.1002/jemt.23139>
- Rehman, A., Khan, M. A., Mehmood, Z., Saba, T., Sardaraz, M., & Rashid, M. (2020). Microscopic melanoma detection and classification: A framework of pixel-based fusion and multilevel features reduction. *Microscopy Research and Technique*, 83(4), 410–423. <https://doi.org/10.1002/jemt.23429>
- Rehman, A., Khan, M. A., Saba, T., Mehmood, Z., Tariq, U., & Ayesha, N. (2021). Microscopic brain tumor detection and classification using 3D CNN and feature selection architecture. *Microscopic Research and Technique*. 128(1):133–149.
- Ronneberger, O., Fischer, P., & Brox, T. (2015) U-net: convolutional networks for biomedical image segmentation. Medical Image Computing and Computer-Assisted Intervention—MICCAI 2015. Lecture Notes in Computer Science. *Medical Image Computing and Computer-Assisted Intervention—MICCAI 2015*.
- Saba, T. (2017). Halal food identification with neural assisted enhanced RFID antenna. *Biomedical Research*, 28(18), 7760–7762.
- Saba, T. (2019). Automated lung nodule detection and classification based on multiple classifiers voting. *Microscopy Research and Technique*, 82(9), 1601–1609.
- Saba, T. (2020). Recent advancement in cancer detection using machine learning: Systematic survey of decades, comparisons and challenges. *Journal of Infection and Public Health*, 13(9), 1274–1289.
- Saba, T., Al-Zahrani, S., & Rehman, A. (2012). Expert system for offline clinical guidelines and treatment. *Life Science Journal*, 9(4), 2639–2658.
- Saba, T., Bokhari, S. T. F., Sharif, M., Yasmin, M., & Raza, M. (2018). Fundus image classification methods for the detection of glaucoma: A review. *Microscopy Research and Technique*, 81(10), 1105–1121.
- Saba, T., Haseeb, K., Ahmed, I., & Rehman, A. (2020). Secure and energy-efficient framework using internet of medical things for e-healthcare. *Journal of Infection and Public Health*, 13(10), 1567–1575.
- Saba, T., Khan, M. A., Rehman, A., & Marie-Sainte, S. L. (2019). Region extraction and classification of skin cancer: A heterogeneous

- framework of deep CNN features fusion and reduction. *Journal of Medical System*, 43, 289. <https://doi.org/10.1007/s10916-019-1413-3>
- Saba, T., Khan, S. U., Islam, N., Abbas, N., Rehman, A., Javaid, N., & Anjum, A. (2019). Cloud-based decision support system for the detection and classification of malignant cells in breast cancer using breast cytology images. *Microscopy Research and Technique*, 82(6), 775–785.
- Saba, T., Mohamed, A. S., El-Affendi, M., Amin, J., & Sharif, M. (2020). Brain tumor detection using fusion of hand crafted and deep learning features. *Cognitive Systems Research*, 59, 221–230.
- Saba, T., Rehman, A., Mehmood, Z., Kolivand, H., & Sharif, M. (2018). Image enhancement and segmentation techniques for detection of knee joint diseases: A survey. *Current Medical Imaging Reviews*, 14(5), 704–715. <https://doi.org/10.2174/1573405613666170912164546>
- Saba, T., Sameh, A., Khan, F., Shad, S. A., & Sharif, M. (2019). Lung nodule detection based on ensemble of hand crafted and deep features. *Journal of Medical Systems*, 43(12), 332.
- Sadad, T., Munir, A., Saba, T., & Hussain, A. (2018). Fuzzy C-means and region growing based classification of tumor from mammograms using hybrid texture feature. *Journal of Computational Science*, 29, 34–45.
- Sajjad, M., Khan, S., Muhammad, K., Wu, W., Ullah, A., & Baik, S. W. (2019). Multi-grade brain tumor classification using deep CNN with extensive data augmentation. *Journal of Computational Science*, 30, 174–182.
- Sandler, M., Howard, A., Zhu, M., Zhmoginov, A., & Chen, L.-C. (2018). MobileNetV2: Inverted residuals and linear bottlenecks. *Proceedings of the IEEE Computer Society Conference on Computer Vision and Pattern Recognition*. doi: <https://doi.org/10.1109/CVPR.2018.00474>
- Seetha, J., & Raja, S. S. (2018). Brain tumor classification using convolutional neural networks. *Biomedical Pharmacology Journal*, 11, 1457–1461.
- Simonyan, K. & Zisserman, A. (2015). Very deep convolutional networks for large-scale image recognition. *3rd International Conference on Learning Representations, ICLR 2015—Conference Track Proceedings*.
- Szegedy, C., Liu, W., Jia, Y., Sermanet, P., Reed, S., Anguelov, D., Erhan, D., Vanhoucke, V., & Rabinovich, A. (2015). Going deeper with convolutions. *Proceedings of the IEEE Computer Society Conference on Computer Vision and Pattern Recognition*. doi: <https://doi.org/10.1109/CVPR.2015.7298594>.
- Szegedy, C., Vanhoucke, V., Ioffe, S., Shlens, J. & Wojna, Z. (2016) Rethinking the inception architecture for computer vision. *Proceedings of the IEEE Computer Society Conference on Computer Vision and Pattern Recognition*. doi: <https://doi.org/10.1109/CVPR.2016.308>.
- Ullah, H., Saba, T., Islam, N., Abbas, N., Rehman, A., Mehmood, Z., & Anjum, A. (2019). An ensemble classification of exudates in color fundus images using an evolutionary algorithm based optimal features selection. *Microscopy Research and Technique*, 82(4), 361–372.
- Viera, A. J., & Garrett, J. M. (2005). Understanding interobserver agreement: The kappa statistic. *Family Medicine*, 37(5), 360–363.
- Yousaf, K., Mehmood, Z., Awan, I. A., Saba, T., Alharbey, R., Qadah, T., & Alrige, M. A. (2019). A comprehensive study of mobile-health based assistive technology for the healthcare of dementia and Alzheimer's disease (AD). *Health Care Management Science*. 2019 1–23.
- Yousaf, K., Mehmood, Z., Saba, T., Rehman, A., Munshi, A. M., Alharbey, R., & Rashid, M. (2019). Mobile-health applications for the efficient delivery of health care facility to people with dementia (PwD) and support to their carers: A survey. *BioMed Research International*, 2019, 1–26.
- Zoph, B., & Le, Q. V. (2017) Neural architecture search with reinforcement learning. *5th International Conference on Learning Representations, ICLR 2017—Conference Track Proceedings*.
- Zoph, B., Vasudevan, V., Shlens, J., & Le, Q. V. (2018) Learning transferable architectures for scalable image recognition. *Proceedings of the IEEE Computer Society Conference on Computer Vision and Pattern Recognition*. doi: <https://doi.org/10.1109/CVPR.2018.00907>

How to cite this article: Sadad T, Rehman A, Munir A, et al.

Brain tumor detection and multi-classification using advanced deep learning techniques. *Microsc Res Tech*. 2021;1–13.

<https://doi.org/10.1002/jemt.23688>